RAYMOND A. GREENWALD, KILE B. BAKER, and J. MICHAEL RUOHONIEMI

EXPERIMENTAL EVALUATION OF THE PROPAGATION OF HIGH-FREQUENCY RADAR SIGNALS IN A MODERATELY DISTURBED HIGH-LATITUDE IONOSPHERE

In March 1987, improvements completed at APL's high-frequency radar in Goose Bay, Labrador, allowed the system to give full information on elevation angle of arrival for all backscattered signals. After several months of calibration and analysis, routine observations were begun. Since October 1987, all data collected by the radar ($\approx$40 Mbytes/day) have been fully processed and stored in an extensive high-frequency-radar database. The data yield new insight into the nature of high-latitude ionospheric irregularities and high-frequency signal propagation in a moderately to severely disturbed ionosphere. In this article we present a sample of these new results, with emphasis on the knowledge gained from the elevation angle-of-arrival observations. Examples have been restricted to daytime observations of ground and ionospheric scatter from the plasma trough, auroral zone, plasma cusp, and polar cap. Our results demonstrate the importance of ionospheric tilts and latitudinally confined electron-density structures in producing anomalous propagation conditions that seriously affect one's ability to relate a given backscatter return to a scatterer at a specific physical location. Examples of anomalous behavior include bifurcation of ground scatter returns, reversals in range versus elevation angle dependencies, and unrealistically high virtual heights for ionospheric irregularity layers.

INTRODUCTION

High-frequency radiowave systems have an extensive history of use in long-distance communications. More recently, systems in this frequency band (3 to 30 MHz) are also finding use in the area of long-distance-radar remote sensing. Frequencies within a significant portion of the high-frequency operating band generally are reflected obliquely from the bottom of the earth's ionosphere and return to the ground at distances of 1000 km and beyond. There, some of the incident energy is backscattered by the terrain and some may be backscattered by targets of interest, such as aircraft or ships. Much of the radar remote sensing at high frequency has been confined to distances—typically 1500 to 3000 km—that involve only a single reflection of the radar signal from the ionosphere, although some extension to either side of these range limits is possible.

In this article, we focus on evaluating the influence of ionospheric structure, particularly tilts and latitudinal variations, on the propagation path of high-frequency radar signals. Studies such as ours should ultimately lead to improvements in target location and clutter mitigation; the two areas are closely related, since one must understand propagation in complex environments to identify correctly the location of the target and to discriminate between returns that have followed radically different propagation paths. Measurements to perform this evaluation were obtained with APL's high-frequency radar at the Air Force Geophysics Laboratory High-Latitude Ionospheric Observatory in Goose Bay, Labrador—an ideal location, since the ionosphere at Goose Bay is affected not only by the daily and seasonal variations in solar illumination, but also by auroral enhancements associated with geophysical disturbances. These enhancements produce unusual ionospheric conditions, such as large-scale structure, tilts, unexpected refraction, and absorption.

The Goose Bay radar is also an ideal instrument with unique features. It can determine the vertical angle of arrival of backscattered signals, thereby allowing evaluation and interpretation of exceedingly complex propagation environments. It also uses an unusual multipulse transmission pattern that enables the autocorrelation function (Fourier transform of the Doppler spectrum) of backscattered signals to be determined without introducing range or frequency aliasing. These features have yielded interesting new observations that should improve our understanding of the proper operation of surveillance radars in less severe, albeit occasionally disturbed, high-frequency-propagation environments.

THE GOOSE BAY RADAR

The APL radar was designed primarily to study the same ionospheric irregularities as those responsible for

ionospheric clutter on long-distance-radar remote-sensing systems. (A detailed description of the original radar can be found in Refs. 1 and 2.) The current configuration of the radar includes several improvements over the original design. The most important, provided largely by the Rome Air Development Center, was the construction of a second array of antennas parallel to and 100 m in front of the original array. (Details of the complex relationship between the azimuthal angle [steering direction] of the radar beam and the phase difference caused by the elevation angle of the backscattered signal are described briefly in an article by Baker and Greenwald elsewhere in this issue.)

The Goose Bay radar uses a multipulse system of seven unevenly spaced pulses. By correlating each pulse with the others, a complete autocorrelation function of 17 lags can be synthesized for every range gate. By lag we mean the unit of time displacement between correlated pulses; the time displacement between any two correlated pulses would be n lags, where n is an integer between 0 and 16 (in this case). Additionally, by correlating the signals received on one array with those received on the other, a similar 17-lag cross-correlation function can be synthesized. Examples of typical auto- and cross-correlation functions are shown in Fig. 1. Although much information can be extracted from these two functions, we focus on four values of major interest in this article: the backscattered power, the mean Doppler velocity, the width of the Doppler power spectrum, and the elevation angle of the received signal.

The Goose Bay radar performs an autocorrelation analysis by scanning through each of the 16 viewing directions, dwelling on each direction for 5 s. During the 5-s integration period, the radar calculates and averages the autocorrelation functions at each range from about 50 multipulse transmissions. On scans for which both autocorrelation and cross-correlation functions are determined, the dwell time on each azimuth is increased to 10 s. This increase is in response to the increased computational time required by the combined auto- and cross-correlation analysis, and it enables these functions to be determined with the same statistical accuracy as that for the autocorrelation function alone. To retain as much temporal resolution as possible in our subsequent analysis, we have adopted an operational scheme in which three scans are completed with only the autocorrelation function being determined, followed by a single scan in which both correlation functions are obtained.

The computer system controlling the Goose Bay radar is a small Data General Micro-Eclipse system with a single 8-in.-reel tape drive. To save magnetic tape and to maintain continuous radar operation throughout the day, the software computes and saves the correlation functions for only the 20 strongest ranges for each 5- or 10-s integration time. Where ground scatter is observed over a very wide range of latitudes, there is a loss of some useful data, but for normal operations the loss is not serious.

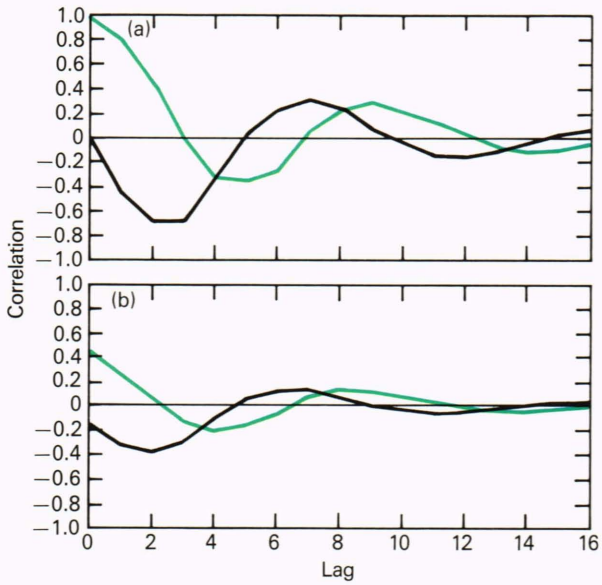

Figure 1—(a) A typical 17-lag complex autocorrelation function of signals backscattered from ionospheric irregularities. The real part (colored line) of the autocorrelation function starts at 1 and the imaginary part starts at 0. Lags are separated by 3 ms. (b) A typical cross-correlation function of ionospheric backscatter received on two antenna arrays. Note that the cross-correlation function phase at zero lag is nonzero.

PRIMER ON HIGH-FREQUENCY PROPAGATION

Before presenting some of our observations, we consider several basic aspects of ionospheric radiowave propagation. For this purpose, it is appropriate to treat the problem from the geometric optics point of view and to consider a flat-earth approximation. The more realistic situation of a curved earth surrounded by an ionospheric shell does not produce any substantive differences in the effects one would observe. In fact, to the lowest order of approximation, the flat-earth analysis is equivalent to a curved-earth analysis with a chord drawn between the point of transmission and the point of ground backscatter. The vertical take-off angle is then the angle between the ray and the chord, rather than the angle between the ray and the local ground.

The simplest examples of ionospheric radiowave propagation are represented in Fig. 2. We have assumed a horizontally stratified ionosphere; Fig. 2a has only an F-layer electron density enhancement and Fig. 2b has both E- and F-layer enhancements. The ray OA in Fig. 2a is known as a "penetrating ray," which has a take-off angle sufficiently high that it cannot be reflected by the ionosphere. Rays OB, OC, and OD are all "reflected rays" that return to the earth. The condition for reflection is obtained from Snell's Law and may be written as

$$\theta_0 \leq \cos^{-1} (1 - f_c^2/f^2)^{1/2} , \qquad (1)$$

where f_c is the critical frequency of the layer, f is the frequency of the transmitter, and θ_0 is the take-off angle of the ray. If ray OB undergoes ground backscatter at the minimum range from the transmitter, it is said

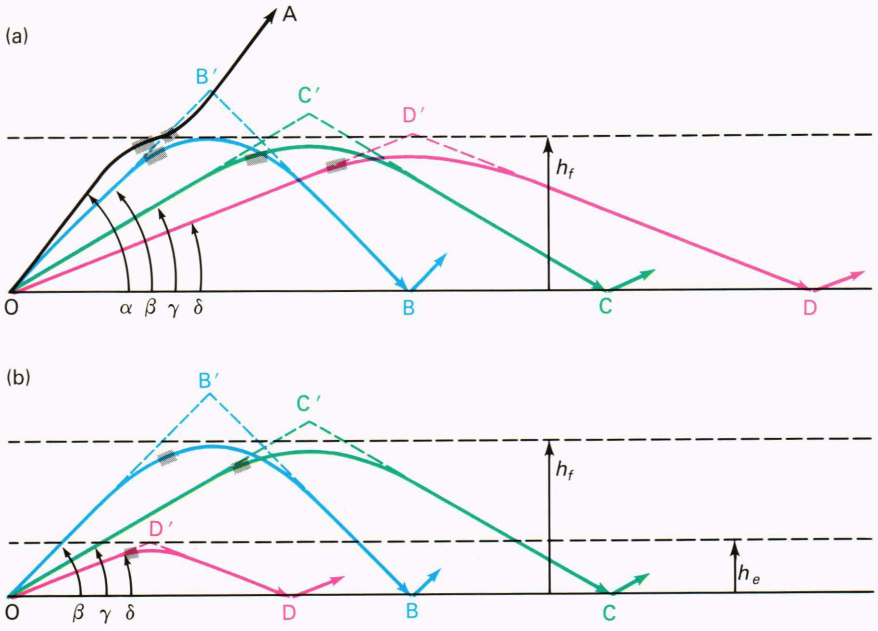

Figure 2—Typical ray paths in the flat-earth approximation of high-frequency signals interacting with a horizontally stratified ionosphere: (a) F layer only, (b) E and F layers (h_e = height of the E-layer maximum, h_f = height of the F-layer maximum).

to be backscattered from the "skip distance," and all other take-off angles will either backscatter from greater ranges or will penetrate the ionosphere. Rays with take-off angles slightly greater than β will propagate for long distances near the layer maximum and will either be reflected toward the ground or penetrate the ionosphere. Those that return to the ground are called "high rays." Because of the wide range of destinations associated with high rays, it is commonly accepted that there is little power in the ground backscatter returns associated with these signals. Although this may be true of the ground backscatter returns, the power density of penetrating wave packets for $\alpha \geq \theta_0 \geq \beta$ may still be large and may contribute to appreciable topside backscatter from ionospheric irregularities.

A consequence of the Breit–Tuve Theorem (see, e.g., Ref. 3) is that the time required for a signal propagating at the velocity of light to transit the path OB′B is identical to the time needed for an ionospheric signal to transit the ray path OB. This result is valid for a horizontally stratified ionosphere and is independent of the vertical ionospheric profile. Point B′ is referred to as the "virtual height" of the apex of the ray. The difference in altitude between the virtual height and the true height of the apex depends on the bottomside ionospheric profile. The true height is generally a small fraction of the virtual height. The virtual height, as well as the penetration depth of the ray, decreases with decreasing θ_0, as shown in Fig. 2a. This result, which is a consequence of Eq. 1, is not quite as severe in the earth's ionosphere, owing to the curvature of the earth.

Figure 2a also illustrates that the propagation time and the ground range associated with any reflected, nonhigh ray increase with decreasing θ_0. This propagation characteristic is valid for both flat and curved geometries and is a feature we expect to observe in our analyses of vertical angle of arrival. The characteristic can be modified, however, if a second ionospheric layer is present. In Fig. 2b, we have assumed an additional E-layer electron density enhancement, which effectively reflects all transmissions with take-off angles

$$\theta_0 < \cos^{-1}\left(1 - [f_E/f]^2\right)^{1/2}, \qquad (2)$$

where f_E is the E-layer critical frequency. In addition to shielding the F layer from lower take-off angle rays, an E layer can cause rays with low take-off angles to have shorter ground ranges than transmissions with higher take-off angles that are reflected from the F layer; in particular, ground scatter returns may be observed within the F-layer skip zone.

The shaded areas along each of the ray paths in Figs. 2a and 2b represent regions where transmissions from the Goose Bay radar are approximately normal to the earth's magnetic field. It is in these regions that the radar is sensitive to backscatter from ionospheric irregularities. For any particular ray, ionospheric backscatter can be observed at slightly less than half the range of the associated ground backscatter return.

We now consider a more complicated situation. Figure 3a shows an ionospheric layer tilted toward the radar, whereas Fig. 3b shows a layer tilted away. The tilts affect the propagation in several ways. They may cause the ground scatter returns for any take-off angle to come from significantly greater or significantly shorter ranges, and the angle of arrival in the target area may be smaller or greater than the take-off angle. Also, the ionospheric layer will have an apparent virtual height that is different from the virtual height for a horizontally stratified ionosphere. Finally, the tilt in Fig. 3a will enable penetrating rays shown in Fig. 2a to be reflected by the ionosphere, whereas the tilt in Fig. 3b will allow reflected rays to penetrate. As a result, small changes within the

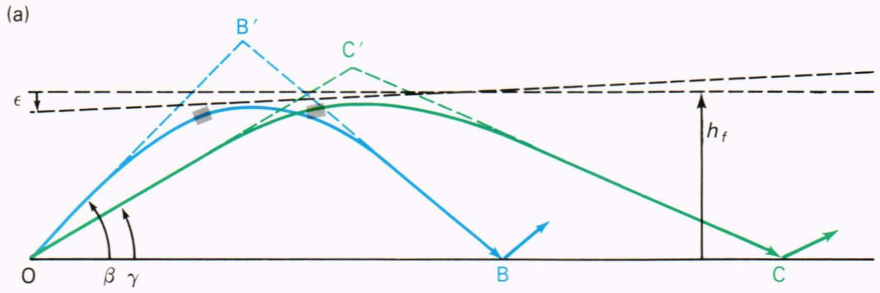

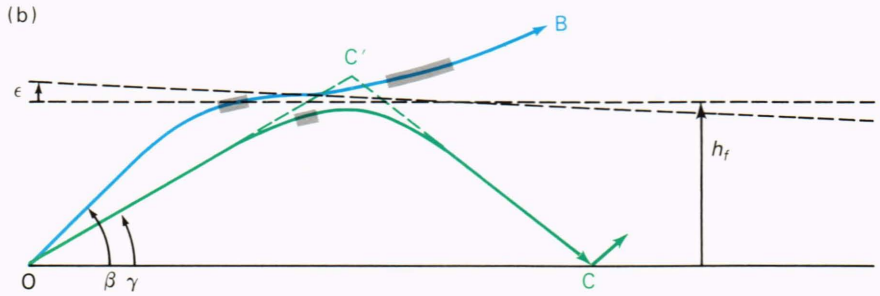

Figure 3—Typical ray paths in the flat-earth approximation of high-frequency signals interacting with a tilted ionosphere: (a) tilted toward the radar, (b) tilted away from the radar.

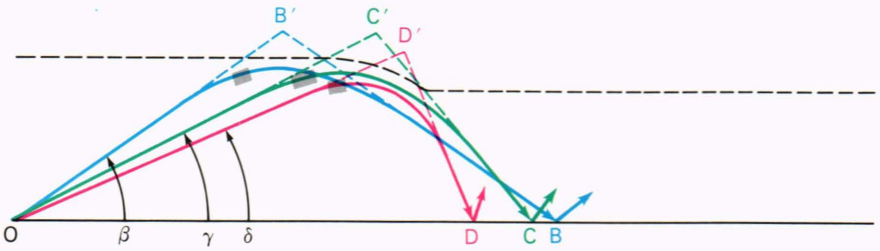

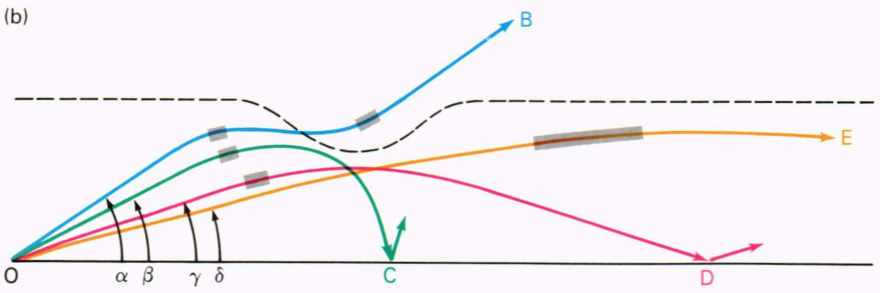

Figure 4—Typical ray paths in the flat-earth approximation of high-frequency signals interacting with a structured ionosphere: (a) abrupt reduction in F-layer height, (b) bulge in F-layer density.

large-scale density structure in the ionosphere may have a dramatic effect on whether a ray is directed toward the skip distance or whether it penetrates and is susceptible to backscatter in the topside ionosphere.

Layer tilts are common within the ionosphere and occur near sunrise and sunset as well as in high-latitude regions where there is oblique incidence of solar illumination. Tilts of even a few degrees can produce significant changes in propagation. Severe tilting of ionospheric layers may create even more marked changes in the propagation environment. Consider, for example, the high-latitude region probed by the Goose Bay radar. At those latitudes, low-energy particle precipitation from the magnetosphere can introduce an F-region density structure of the type shown in Fig. 4. We have assumed in Fig. 4a that the precipitation has produced a decrease in layer height and that none of the rays penetrate the layer. Under these conditions, which are somewhat anomalous and opposite to those shown in Fig. 2a, it is possible to force the rays with lower take-off angles to have shorter propagation paths and propagation times. Figure 4b shows a spatially confined density enhancement protruding from the bottom of the F layer, where ray OB penetrates the ionosphere and may be backscattered by topside ionospheric irregularities. Rays OC, OD, and OE are all reflected by the ionosphere. For relatively small changes in take-off angle there are extremely large variations in the ground range of the reflected rays.

RESULTS

Using the foregoing propagation primer as a point of reference, we now focus on examples of recent daytime observations (1200 to 2200 UT) with the Goose Bay radar. The selected examples include both ground and ionospheric backscatter, and exhibit many of the characteristics previously reviewed.

We first examine ground scatter observed during the afternoon of 9 September 1987. Figures 5a and 5b show maps of the lag-0 power and the elevation angle, respectively. Significant backscattered power was present at nearly all ranges for the entire scan, as shown in Fig. 5a. Note that the geographical location of the data being displayed is the location of the ground scatter point, not the location of the reflection point. Because the radar microcomputer determines only full autocorrelation functions for the 20 strongest ranges on each beam, the elevation angle map shown in Fig. 5b presents only results for those ranges. The elevation angle results clearly exhibit a decrease in angle of arrival with increasing range, in agreement with our discussions based on Fig. 2a.

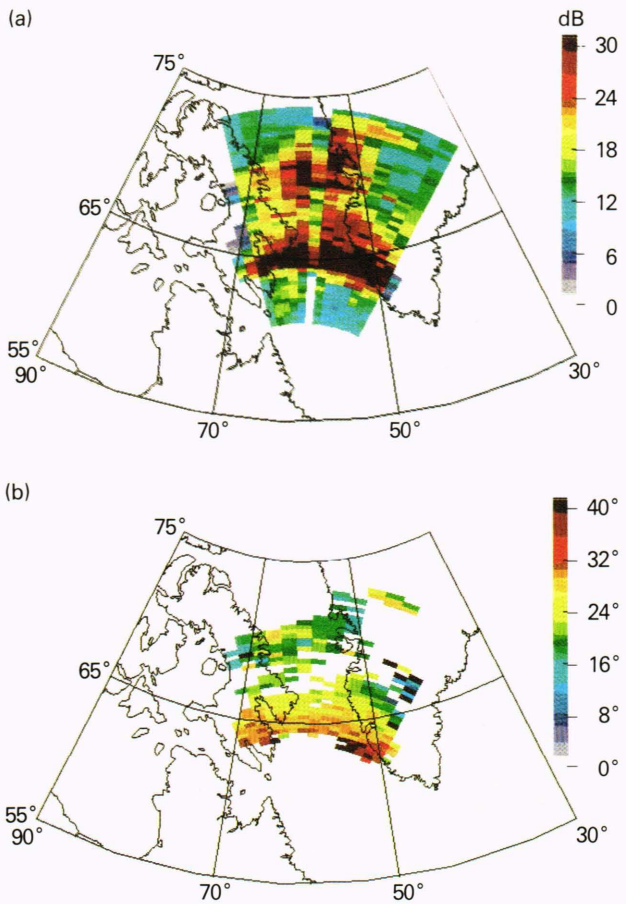

Figure 5—Maps of (a) the lag-0 power and (b) the elevation angle for the scan beginning at 2025:40 UT on 9 September 1987 (frequency = 11.3 MHz). The position corresponds to the ground scatter point, not the ionospheric reflection point. The backscattered power ranges from 0 to 30 dB, and the elevation angle ranges from 0 to 40°.

In Fig. 6a we show a more detailed plot of the elevation angles measured along beam 8. The horizontal bars at each data point represent the horizontal resolution of the measurement (30 km), and the vertical bars reflect the error in the angle-of-arrival determination. For the better data points, the error is typically less than 1°. Using a curved-earth model and the data in Fig. 6a, we have also been able to determine the virtual height of the ionospheric reflection point. The results, shown in Fig. 6b, indicate a relatively constant reflection height of about 350 km. While this virtual altitude will always be greater than the true altitude, the difference between the virtual height and the true height will be small if the ionospheric density builds up rapidly as the altitude increases. Also, the virtual altitude is typical of what one would expect for a reflection originating near the F-region maximum.

The ionosphere was quite stable during the observation period, and the ground backscatter continued until late afternoon. The K_p magnetic index ranged between 1 and 2^-, indicating relatively quiet magnetic conditions.

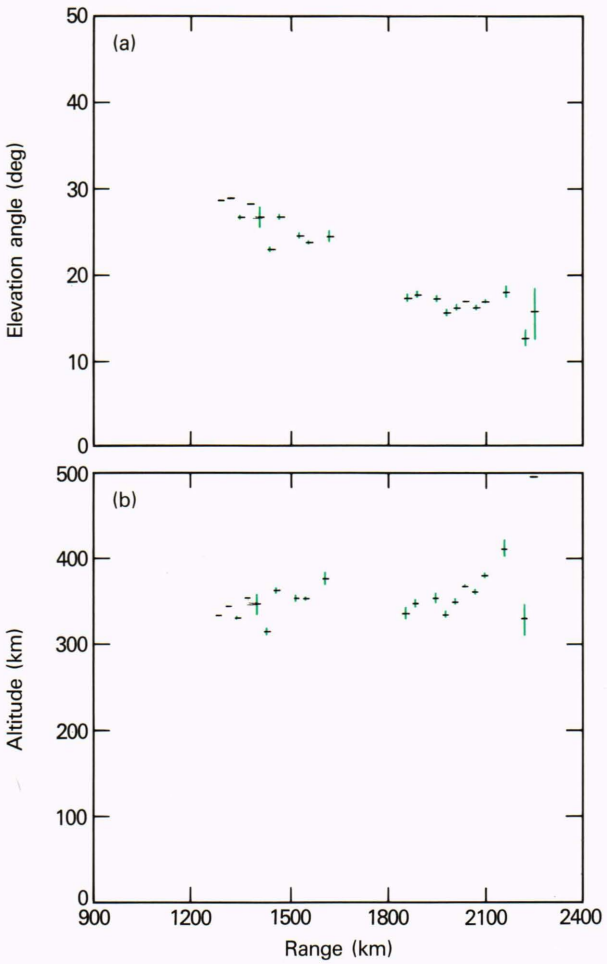

Figure 6—(a) A plot of elevation angle versus range for ground backscatter returns on 9 September 1987 at 2027 UT (frequency = 11.4 MHz). Range resolution is given by the horizontal bars, error in elevation angle by the vertical bars. (b) A plot of virtual height of the ionospheric reflection versus range. Range resolution is given by the horizontal bars, altitude resolution by the vertical bars.

Starting about 2200 UT, a region of ionospheric clutter appeared at the nearer ranges. Figures 7a and 7b show maps of the Doppler velocity and elevation angle at that time. Since the reflection point for ground scatter in a horizontally stratified ionosphere is at half the range of the ground scatter point, the reflection is approximately co-located with the ionospheric clutter, but originates from rays with larger take-off angles that penetrate deeper into the F layer (a situation analogous to that shown in Fig. 2a).

Although individual images of the data obtained from scans of the Goose Bay radar are of interest, one can gain an even better understanding of the temporal dynamics of high-latitude propagation by considering the time series of various radar parameters along a single radar azimuth. The following data will be presented along beam 8, which is directed about 6.5° to the east of geographic north. We begin with examples of relatively quiescent events that exhibit predominantly ground backscatter.

Figure 8 shows the power, elevation angle, and Doppler velocities of ground backscatter returns observed on 9 October 1987, which was a very quiet magnetic period (K_p = 0). The range of the ground scatter return decreases during the day as the ionospheric density increases in response to solar extreme-ultraviolet illumination. Along with this density increase, rays with higher take-off angles are reflected by the ionosphere as the day progresses. Although there is some modulation in the angle of arrival at any given range, possibly as a consequence of gravity-wave or traveling ionospheric disturbance phenomena, the gross behavior is that angles of arrival above 30° are generally observed inside a 1400-km range, and smaller angles are observed beyond. This example of ionospheric propagation clearly shows that there is a concentration of transmitter signal near the skip distance and that the angle of arrival decreases with range as one would expect in a simple situation. An interesting splitting of the echo returns occurs sporadically between 1400 and 1600 UT. This splitting produces a region between about 1500 and 1700 km in which no echoes are observed, and it may be a consequence of latitudinal electron density structure in the F region near the reflection point or in the E region along the path of the downgoing rays. Another salient feature is the thin region of ground backscatter observed at about 1000 km in range. Although it is not clear in the example shown in Fig. 8, these returns are presumably caused by an E-region reflection mode. The take-off angles for these rays are about 12°.

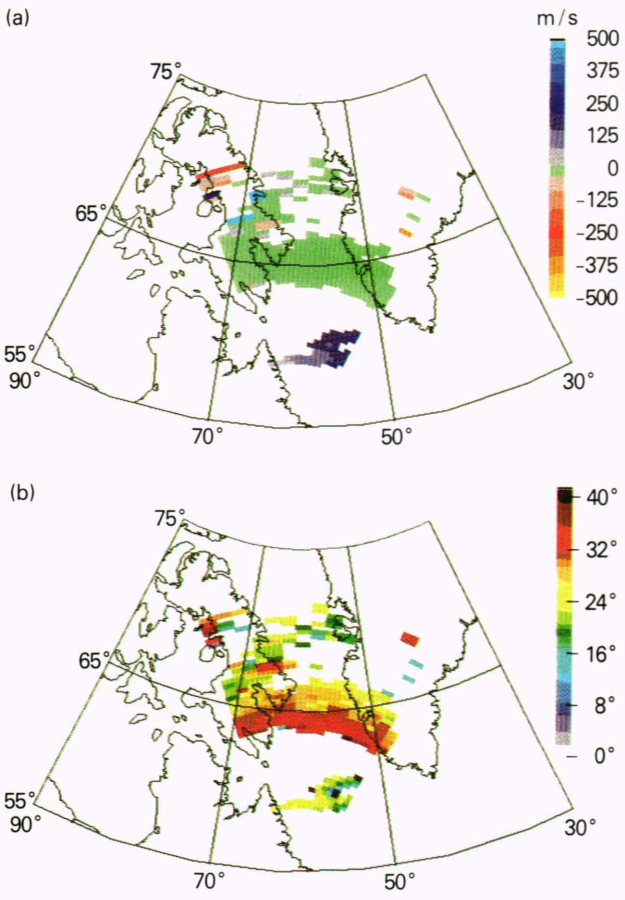

Figure 7—Maps of (a) the Doppler velocity and (b) the elevation angle for the scan beginning at 2200:50 UT on 9 September 1987 (frequency = 11.3 MHz).

The Doppler velocity data for the 9 October 1987 event are also distinctive. On the ±30-m/s velocity scale (Fig. 8d), a generally negative Doppler shift of about 5 m/s occurs for the equatorward portion of the ground scatter returns. This shift indicates a gradually increasing path length. Conversely, the poleward portion of the backscatter exhibits a 5-m/s positive Doppler shift, indicating a gradually decreasing path length. One would nominally expect only positive Doppler shifts during periods of ionospheric buildup and only negative Doppler shifts during periods of ionospheric decay. The bifurcation in Doppler shift is, therefore, quite unusual.

We now examine pure ionospheric scatter, with no evidence of ground scatter. The most dynamic region for daytime ionospheric backscatter is the polar cusp or cleft, which is normally located near local noon at magnetic latitudes of 75° (≈ 65° geographic in northeastern Canada and Greenland). Although controversy continues over the precise definition of the polar cusp, we shall refer to it as the region within 2 h of magnetic local noon, where the plasma flow changes from sunward to antisunward and a significant poleward component to the velocity vectors occurs. The period from 1400 to 1500 UT on 13 September 1987 (K_p = 4) is a good example of this behavior. Figure 9 shows the data for the scan starting at 1434:45 UT (≈ 1130 MLT). The Doppler velocity map (Fig. 9b) illustrates two distinct regions, one with large negative Doppler velocities (up to nearly 1000 m/s) and another toward the magnetic east with smaller positive velocities. The spectral width map (Fig. 9d) indicates that the Doppler spectrum for both regions is generally quite wide, with some half-power widths greater than 500 m/s. Examples of power spectra obtained along beam 5 are shown in Fig. 10. Some of these spectra are so wide that there is a significant amount of back-

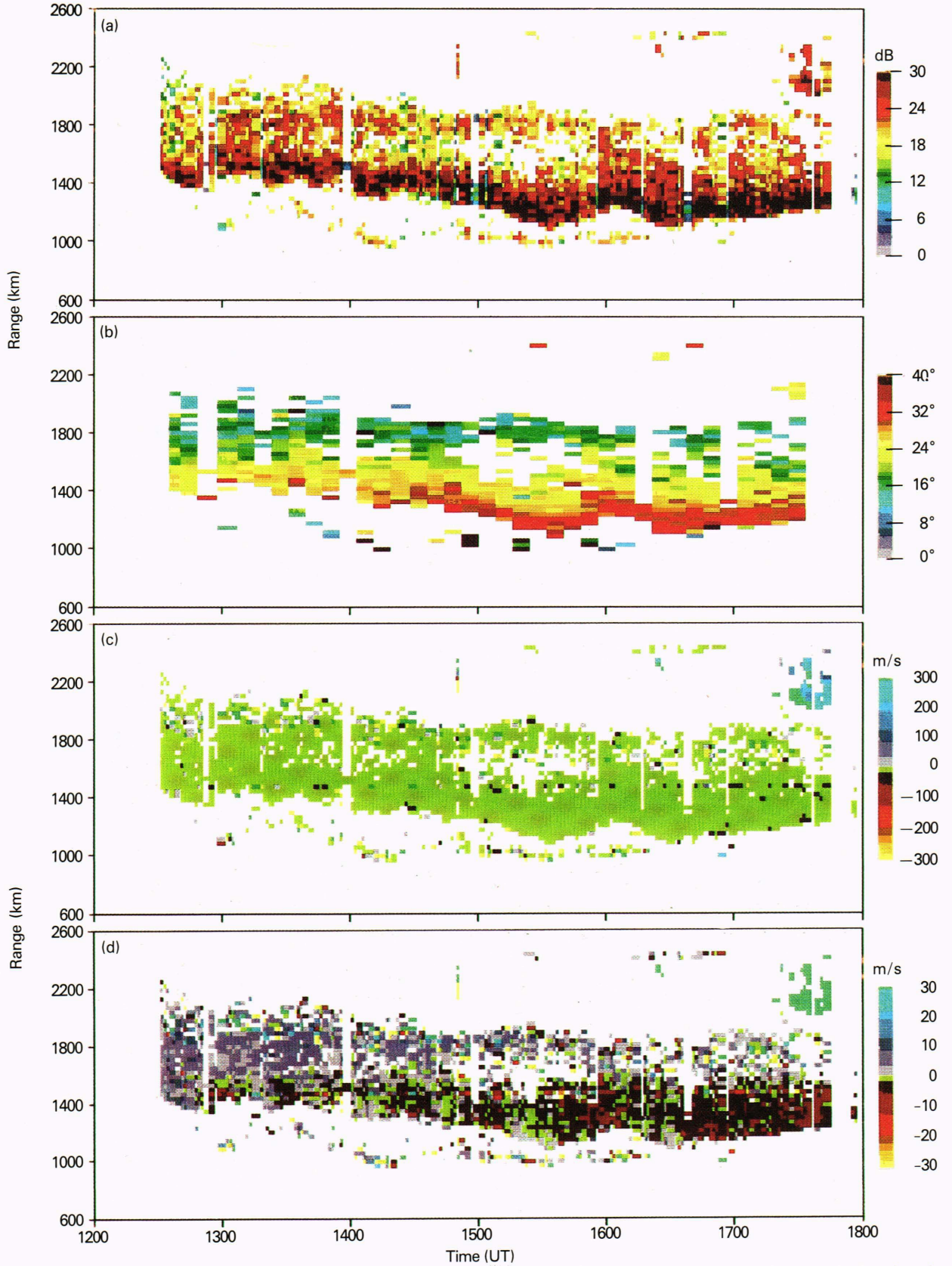

Figure 8—Time-series plots (time runs from 1200 to 1800 UT on 9 October 1987) of (a) the backscattered power, (b) the elevation angle, (c) the Doppler velocity, with a scale from −300 to +300 m/s, and (d) the Doppler velocity with a scale from −30 to +30 m/s. The data are taken from a single azimuth (beam number 8) pointing about 6.5° east of geographic north (frequency = 11.5 MHz). The coarseness in the time resolution of the elevation angle data occurs because cross-correlation scans are made only every fourth scan.

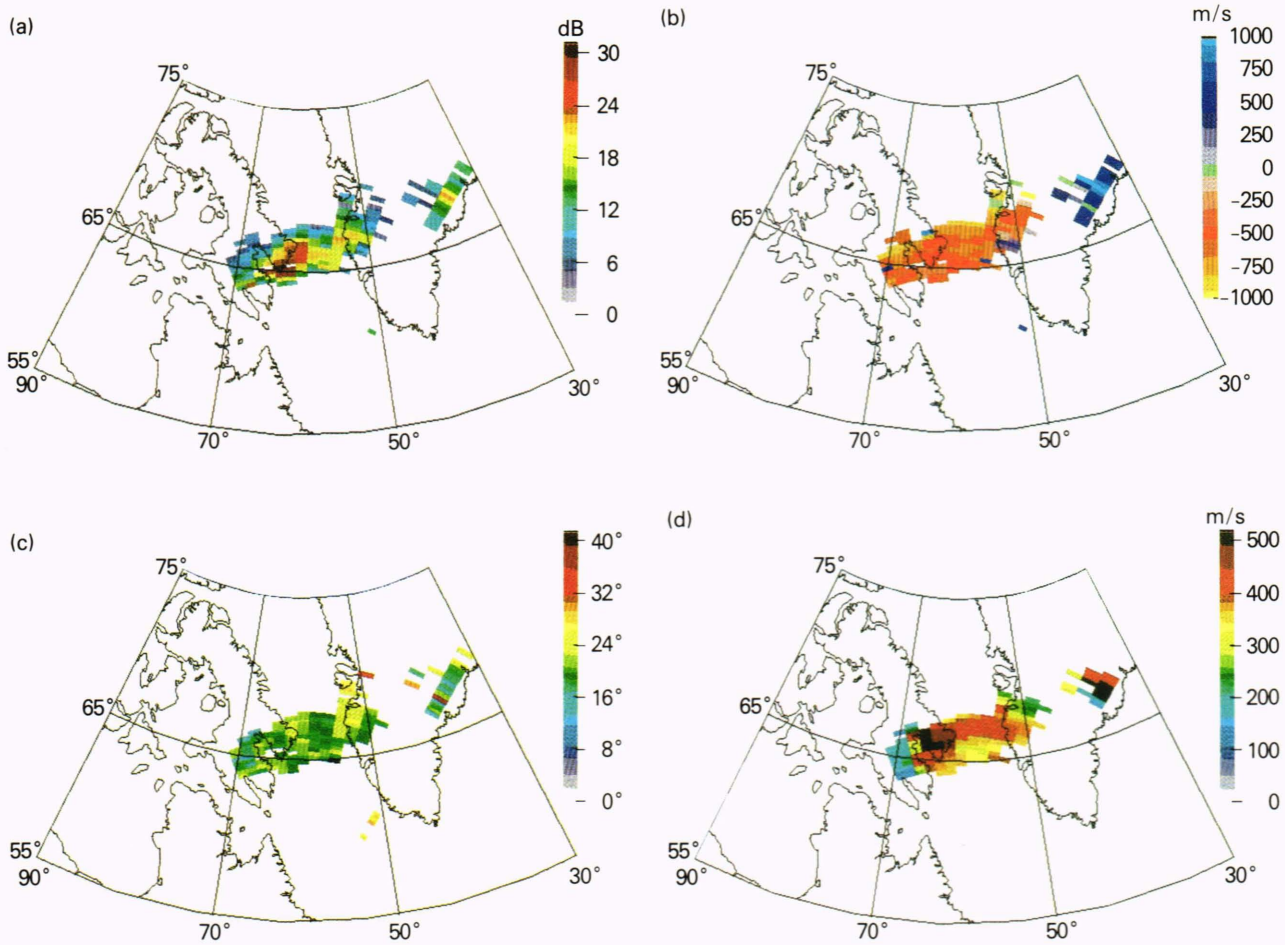

Figure 9—Maps for (a) the backscattered power, (b) the Doppler velocity, (c) the elevation angle, and (d) the spectral width for the scan beginning at 1434:45 UT on 13 September 1987 (frequency = 11.5 MHz).

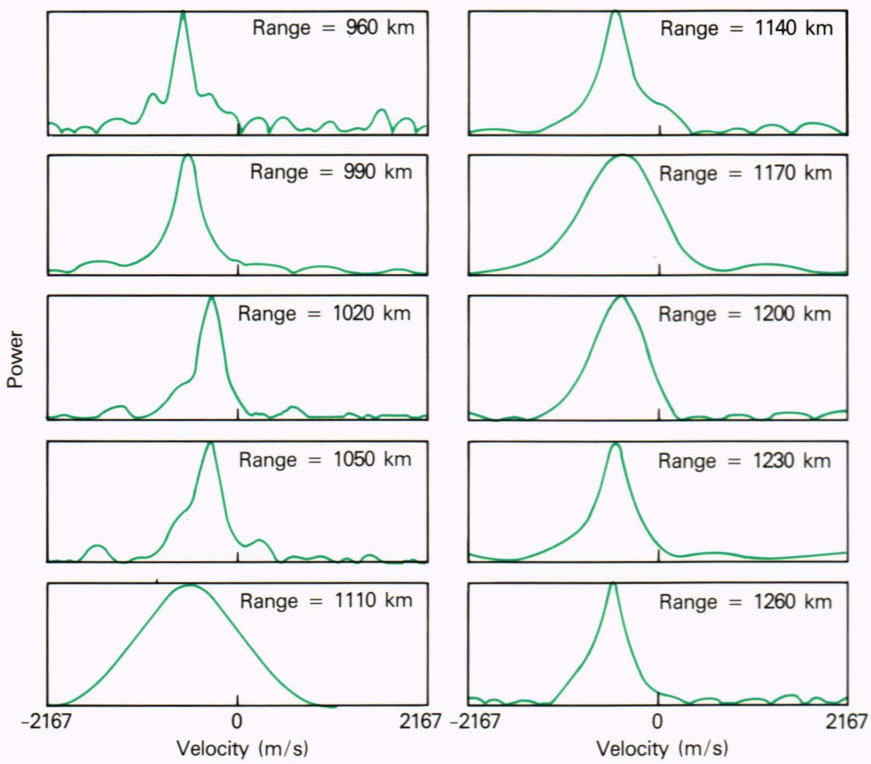

Figure 10—Examples of Doppler spectra determined from the Fourier transformation of autocorrelation functions obtained on 13 September 1987 at 1435:35 UT (frequency = 11.5 MHz).

scattered power at positive Doppler velocities, even though the mean Doppler velocity is negative. In fact, if a radar, operating at 11.5 MHz, were to sample the backscattered signals at a 50-Hz rate, the spectra would be aliased totally and would appear as an overall enhancement of the system noise level.

The elevation angles for the 1434:45 UT scan (Fig. 9c) are about 20°; on several beams, the angle increases with range, rather than exhibiting the anticipated decrease. Figures 11a and 11b show the elevation angle and virtual height, respectively, for beam 5. The virtual heights, ranging from about 500 to over 800 km, are all much larger than can be expected for the true height, and probably indicate that the rays are penetrating the ionosphere. Because of the long distance the rays can travel before they penetrate the F-region maximum and begin to steepen, the virtual height becomes very large, even though the true height may be only slightly above the F-region maximum (e.g., ray OB in Fig. 3b).

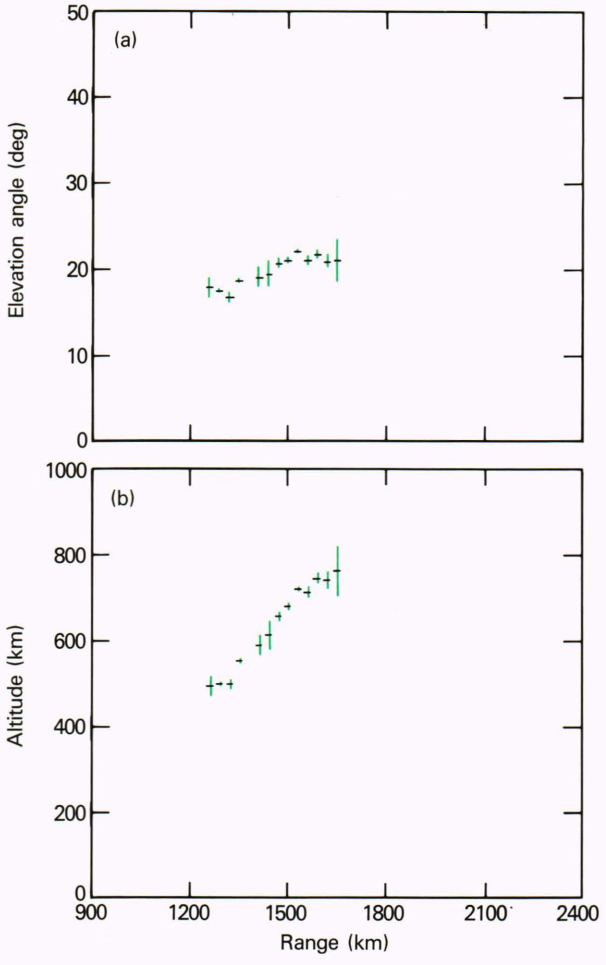

Figure 11—(a) A plot of the elevation angle versus range for ionospheric backscatter returns on 13 September 1987 at 1435:35 UT (frequency = 11.5 MHz). Error bars have the same meaning as in Fig. 6a. (b) A plot of virtual height of the ionospheric scattering layer versus range. Note the rapid increase of virtual height with range. Error bars have the same meaning as in Fig. 6b.

Figure 12 represents a 4-h time series of power, elevation angle of arrival, and Doppler velocities for 24 October 1987, covering the afternoon and evening local time sectors. Early in the event, the backscatter condition is similar to the ground backscatter conditions noted above (K_p was a moderate 2^+). Strongly bifurcated ground backscatter via a 1-hop F-region mode occurs at ranges of 1300 km and beyond, and maximum elevation angles are about 32°. There is also evidence of a 1-hop E-region mode at a range of 1200 km. The bifurcation coalesces into a single ground backscatter region at 1700 UT. It remains in this form until shortly before 1800 UT, when the ground backscatter is replaced by ionospheric backscatter in the range interval from 1400 to 1800 km. Also, K_p increases dramatically from 2^+ to 5^-, indicating the occurrence of a large magnetic disturbance. The ionospheric backscatter is at least as intense as the ground backscatter that immediately preceded it. The scattering region first exhibits negative Doppler velocities of 300 m/s, but as the scattering region moves equatorward, the Doppler motions become positive and approach 400 m/s.

Elevation angle changes are perhaps the most interesting aspect of the transition from ground scatter to ionospheric scatter. Before the transition, the elevation angle varied from 30 to 32° for scatter returns from 1600 km in range. Afterward, ionospheric scatter from the same range exhibited elevation angles of about 18°. The virtual height of the reflecting layer is approximately 460 km for the ground scatter returns; the virtual height of the scattering layer is nearly 700 km for the ionospheric returns. Both of these values are high. The reflection height may be explained by a slight ionospheric tilt; the scattering height may be explained by assuming that the scattering occurs on the topside of the ionosphere (see the discussion of Fig. 9).

Note also in Fig. 12 the apparent continuance of high ($\approx 30°$) elevation angles from the poleward edge of the region of ionospheric scatter. Examination of the Doppler velocities indicates that at least some of the returns from this region are caused by ground backscatter. Presumably, the 1-hop F region is still active for these ranges and possibly also for the shorter ranges where ionospheric scatter is observed. The ionospheric return dominates the analysis, however, because of its greater signal power.

Another example of a transition from ground scatter to ionospheric scatter is presented in Fig. 13. The data for this event were obtained in the local afternoon of 3 November 1987 (for beam 8) when the magnetic conditions were disturbed ($K_p = 5^+$). The event is particularly significant both for its complexity and for the manner in which it demonstrates the importance of elevation angle measurements. From the Doppler data (Figs. 13c and 13d), one sees that the radar returns are dominated by ground scatter before 1700 UT. All of these ground returns appear to be caused by 1-hop F modes. The largest angles of arrival approach 40°. At the farthest range, there is also evidence of a 1½-hop ionospheric scatter mode, with a virtual height of 470 km and a ground reflection point occurring just inside 1400 km.

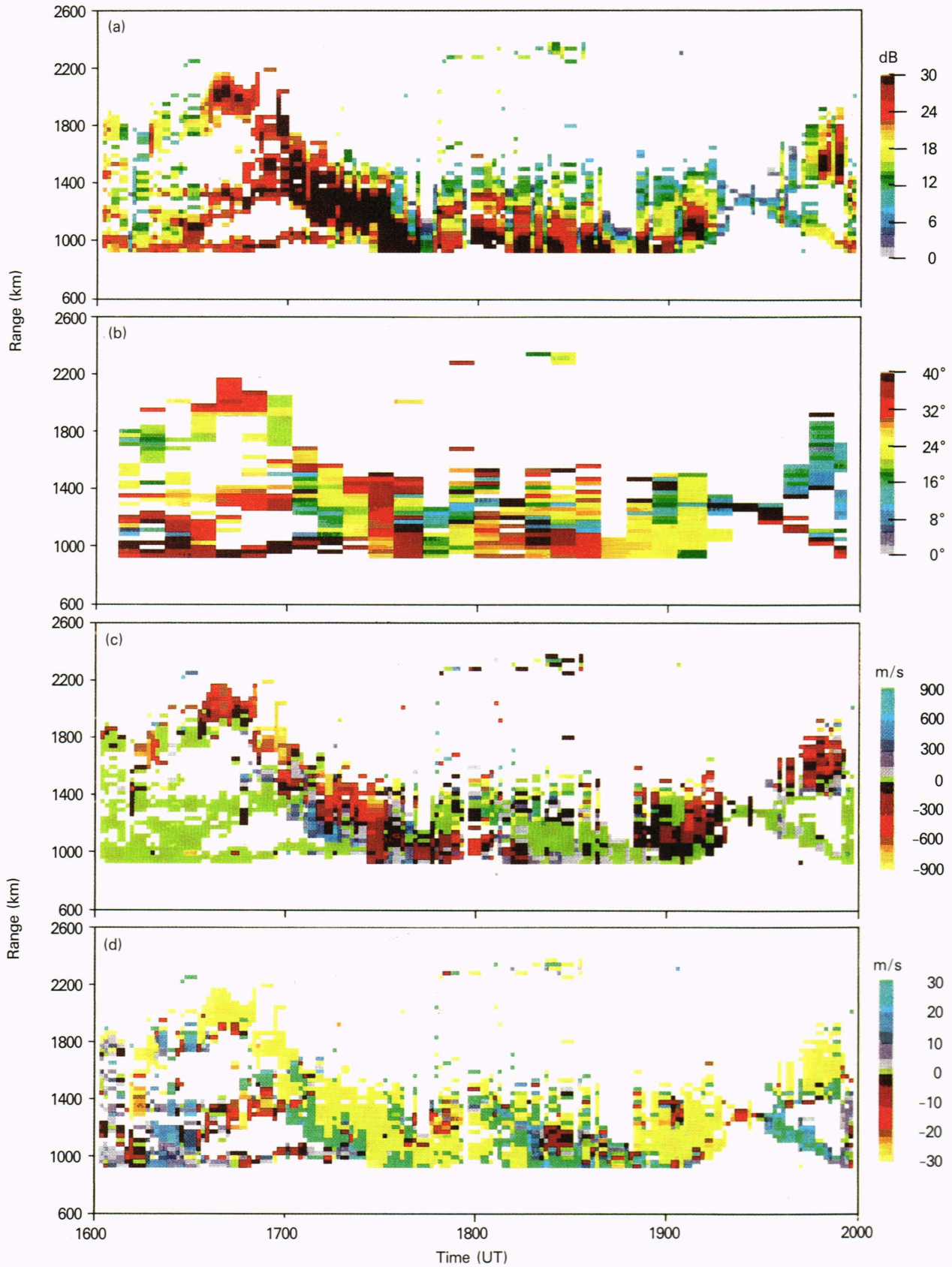

Figure 12—Time-series plots of (a) the backscattered power, (b) the elevation angle, (c) the Doppler velocity with a scale from −600 to +600 m/s, and (d) the Doppler velocity with a scale from −30 to +30 m/s for the period from 1600 to 2000 UT on 24 October 1987 along beam number 8 (frequency = 11.5 MHz).

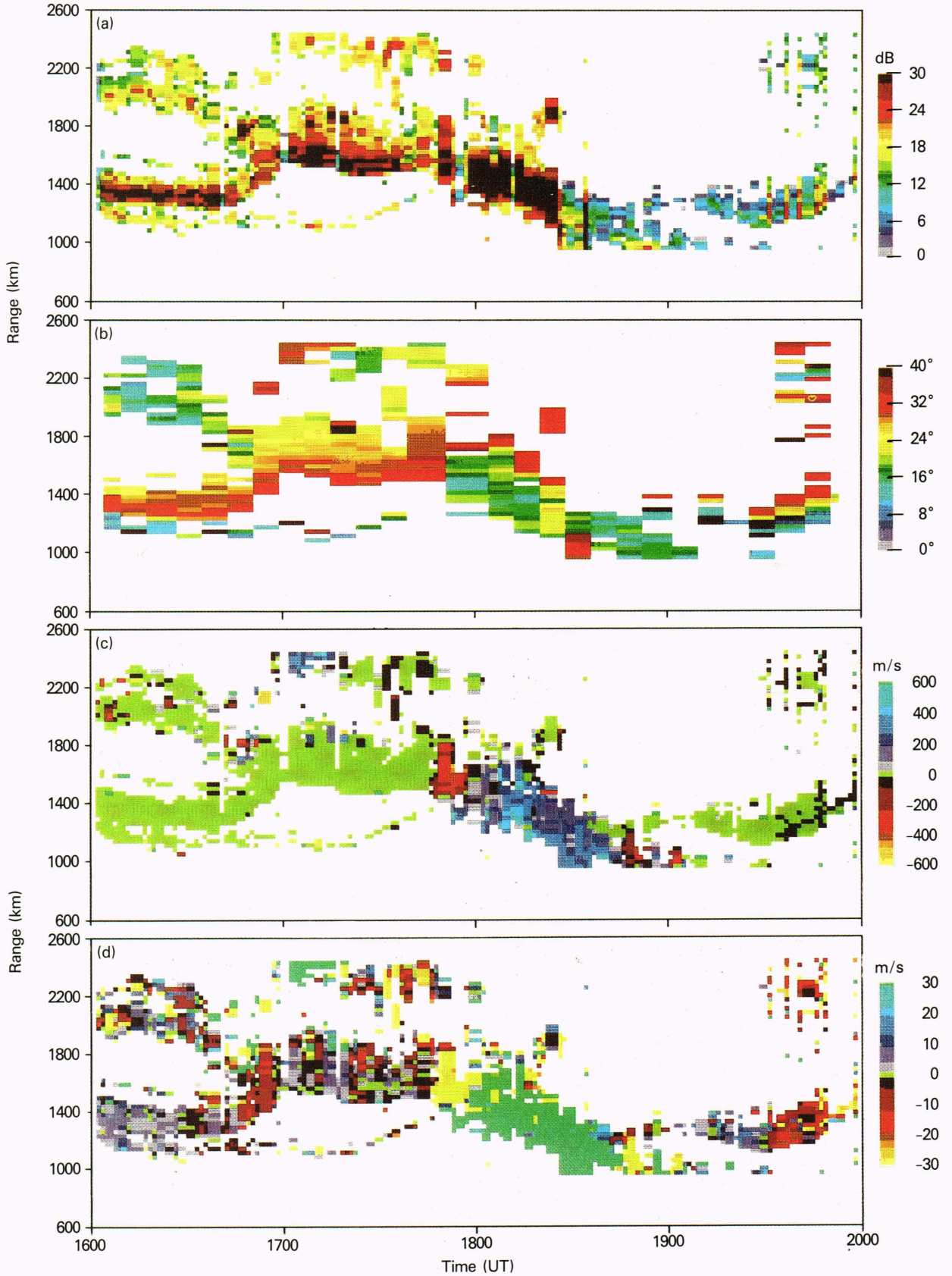

Figure 13—Time-series plots of (a) the backscattered power, (b) the elevation angle, (c) the Doppler velocity with a scale from −900 to +900 m/s, and (d) the Doppler velocity with a scale from −30 to +30 m/s for the period from 1600 to 2000 UT on 3 November 1987 (frequency = 11.3 MHz).

After 1700 UT, the ionospheric scatter intensifies and moves rapidly equatorward. Except for the period from 1815 to 1850 UT, ionospheric scatter dominates the returns until 1920 UT. During most of the intervening period, the elevation angle of the ionospheric scatter is about 20°, implying that the virtual height of the scattering layer ranges from 400 to 500 km. The notable exception to this general behavior occurs in the period around 1730 UT, when intense ionospheric irregularities with elevation angles of 35 to 38° are observed. If these returns were caused by direct ionospheric backscatter, their virtual heights would exceed 900 km. A detailed analysis of the full scans for this period indicates that an alternative explanation is more likely; that is, the high-angle ionospheric backscatter results from a 1½-hop propagation mode. One important consequence of this analysis is that between 1720 and 1740 UT two distinct ionospheric scatter modes may have coexisted over a significant portion of the backscatter image. These modes have very different elevation angles (≈ 20 and $\approx 38°$) and presumably are associated with ionospheric scatter that is more intense than any coexisting ground scatter mode from the same range interval. Since the coexisting ground scatter would probably have an elevation angle somewhere between 20 and 38°, it is extremely difficult to separate the ground scatter return from the extant ionospheric modes.

SUMMARY

The observations presented in this article are a small, but interesting, sampling of the results being obtained with APL's Goose Bay radar. This radar can resolve the elevation angle of arrival of backscattered signals from the ionosphere and from the ground. It can also determine with certainty the range and spectral dependence of the backscattered signals. In effect, we now can perform a detailed analysis on each propagation mode occurring in a complex high-frequency-propagation environment. The analyses could not have been performed without the restrictions imposed by the elevation angle measurements.

Our measurements indicate that under undisturbed ionospheric conditions the propagation environment is very similar to that expected from a horizontally stratified ionosphere. Specifically, the altitude of reflection of high-frequency signals is consistent with that expected in the ionosphere, the elevation angles of reflected signals are also consistent with concurrent F-region peak electron densities, and the range of ground scatter returns increases with decreasing elevation angle. But as soon as processes are introduced that produce ionospheric tilt and, more important, latitudinal ionospheric structure, the propagation environment becomes extremely complex. Significant disturbance-producing processes may occur anywhere from the ionospheric trough to the polar cap. They may be associated with both electron and ion precipitation processes, as well as with ionospheric plasma transport.

In our analysis of high-frequency-radar backscatter, we have found (1) unusual variations in the rate of change of the group path of ground scatter returns, (2) examples of both ground scatter returns and ionospheric scatter returns for which the elevation angle of arrival increases (rather than decreases) with increasing group range, (3) many examples of apparent topside ionospheric backscatter, and (4) examples of multimode ground scatter and multimode ionospheric scatter from common or near-common viewing areas.

Although there is a tendency to be overwhelmed by the various forms of anomalous propagation, a survey of the much larger database indicates that many of our observations are simply different manifestations of a relatively small number of basic ionospheric conditions. The fundamental pattern may be a normal ionosphere and a latitudinally confined electron-density enhancement or depression that extends through the F region, the E region, or both.

ACKNOWLEDGMENTS—This work was supported in part by the Defense Nuclear Agency and the Rome Air Development Center under Contract N00039-87-C-5301. The Goose Bay high-frequency radar is supported in part by the National Science Foundation (NSF) Division of Atmospheric Sciences and the Air Force Office of Scientific Research, Directorate of Atmospheric and Chemical Sciences, under NSF grant ATM-8506851. The authors would like to thank J. Kelsey and his co-workers for their help in the day-to-day operations of the Goose Bay radar, and the Ionospheric Branch of the Air Force Geophysics Laboratory for permission and support in operating from its Goose Bay field site.

THE AUTHORS

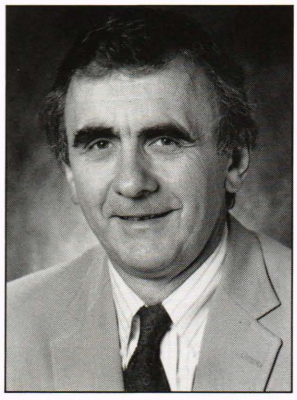

RAYMOND A. GREENWALD was born in Chicago in 1942. He received an undergraduate degree from Knox College and a Ph.D. degree in physics from Dartmouth College in 1970, specializing in laboratory plasma physics. After completing a postdoctoral fellowship studying laboratory plasmas at NOAA's Environmental Research Laboratory in Boulder, Colo., he continued working there, using ground-based radars to study plasma instabilities in the ionosphere.

Between 1975 and 1979, Dr. Greenwald worked at the Max Planck Institute in Lindau, West Germany, where he was responsible for developing several very-high-frequency radars that were used to provide new information on plasma processes in the ionosphere over northern Scandinavia.

Since 1979, Dr. Greenwald has worked at APL, where he has led the development of scientific high-frequency radar systems used to detect small-scale ionospheric irregularities in the auroral zone and the polar cap. He has been responsible for APL's high-frequency radar located at Goose Bay, Labrador, and, more recently, he has been U.S. principal investigator on the PACE high-frequency radar constructed in conjunction with the British Antarctic Survey at Halley Bay, Antarctica.

Dr. Greenwald is a member of the Principal Professional Staff and is a Section Supervisor in the Space Physics Group of the Space Department.

KILE B. BAKER's biography can be found on p. 130.

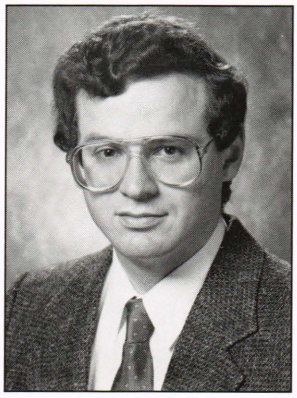

J. MICHAEL RUOHONIEMI was born in 1958 in Prince Edward Island, Canada. He received B.A. and B.Sc. degrees from the University of King's College, Dalhousie, in 1981 and graduated with a Ph.D. in physics from the University of Western Ontario in 1986. His dissertation research dealt with the characteristics of small-scale ionospheric irregularities at high latitudes. Dr. Ruohoniemi joined the Ionospheric Physics Section of APL's Space Physics Group as a postdoctoral research associate in 1986. He is now studying irregularity formation and plasma dynamics in the high-latitude ionosphere with APL's high-frequency radar at Goose Bay, Labrador.